3-HYDROXYANTHRANILIC ACID INTESTINAL LOCALIZATION AND IMMUNE FUNCTION IN *CAENORHABDITIS ELEGANS*.

by

Anne Haskins

A Thesis Submitted to the Faculty of the

GRADUATE INTERDISCIPLINARY PROGRAM IN GENETICS

In Partial Fulfillment of the Requirements
For the Degree of

MASTER OF SCIENCE

In the Graduate College

THE UNIVERSITY OF ARIZONA

2024

THE UNIVERSITY OF ARIZONA
GRADUATE COLLEGE

As members of the Master's Committee, we certify that we have read the thesis prepared by Anne Elizabeth Haskins, titled *3-hydroxyanthranilic Intestinal Localization and Immune Function in Caenorhabditis elegans* and recommend that it be accepted as fulfilling the dissertation requirement for the Master's Degree.

George Sutphin — Date: 4/15/24
George Sutphin, Chair

Michael David Leslie Johnson — Date 4/15/24
Michael Johnson, Committee Member

Ted Weinert — Date: 4/15/24
Ted Weinert, Committee Member

Final approval and acceptance of this thesis is contingent upon the candidate's submission of the final copies of the thesis to the Graduate College.

I hereby certify that I have read this thesis prepared under my direction and recommend that it be accepted as fulfilling the Master's requirement.

George Sutphin — Date: 4/15/24
George Sutphin
Master's Thesis Committee Chair
Genetics Graduate Interdisciplinary Program

Signature: George Sutphin
Email: sutphin@gmail.com

Signature:
Email: mdljohnson@arizona.edu

Signature: Ted Weinert
Email: tweinert@arizona.edu

LAND ACKNOWLEDGEMENT

We respectfully acknowledge the University of Arizona is on the land and territories of Indigenous peoples. Today, Arizona is home to 22 federally recognized tribes, with Tucson being home to the O'odham and the Yaqui. Committed to diversity and inclusion, the University strives to build sustainable relationships with sovereign Native Nations and Indigenous communities through education offerings, partnerships, and community service.

TABLE OF CONTENTS

LIST OF FIGURES

ABSTRACT

Aging is experienced by most eukaryotic organisms and age is the primary risk factor for many of the most common causes of death in humans. Age-related diseases not only increase risk of death in older adults, but significantly reduce their quality of life. Aging research is focused on understanding the molecular processes that drive age-associated decline with the goal of both extending lifespan and improving overall health. Recently, the kynurenine pathway, the primary tryptophan metabolic pathway, has proven to be a potential target for increasing both lifespan and healthspan. The kynurenine metabolite 3-hydroxyanthranilic acid (3HAA) has been shown to extend lifespan in *C. elegans* and in mice. Additionally, 3HAA exhibits antibiotic effects in liquid *E. coli* culture and increases pathogen resistance in worms. 3HAA co-localizes with bacteria in lysosome-related organelles (LROs) called gut granules in the worm intestine, providing a physical location at which 3HAA may directly inhibit bacterial growth *in vivo*. Gut granules have several biological roles, including the sequestration and storage of intracellular zinc. While 3HAA clearly accumulates in gut granules, the 3HAA trafficking mechanisms have yet to be determined. Through this work I aim to determine the molecular processes that transport 3HAA to the gut granule as well as characterize the immune function of 3HAA and stored zinc within the worm gut granule. I found that 3HAA is likely using vesicular transport to travel to LROs. Additionally, the combination of zinc and 3HAA treatment in *E. coli* liquid culture increases 3HAA's existing antibiotic effect.

INTRODUCTION

Aging is conserved amongst most eukaryotic organisms and can lead to a variety of age-related diseases that decrease quality of life in older adults. It is therefore of interest to discover ways to combat age-related disease and improve overall health as we age. The kynurenine pathway, or the primary tryptophan metabolic pathway, has been shown to be a potential target for lifespan extension. Previous research shows that the kynurenine metabolite 3-hydroxyanthranilic acid (3HAA) extends lifespan in *Caenorhabditis elegans* and mice.[1] In this thesis, I explore the benefits of 3HAA in immune response and bacterial pathogen resistance during aging. I specifically investigate the role of 3HAA localization within the worm intestine in pathogen resistance. 3HAA and bacteria appear to co-localize in small granule-like organelles in the gut, providing a possible physical location within the intestine where 3HAA and pathogens interact. I aim to characterize the potential mechanism of transport for 3HAA to these granules as well as its impact on bacterial growth *in vitro*.

I. Physiological function declines with age.

Between 2018 and 2021, the top 3 causes of death in older adults were heart disease, cancer, and COVID-19.[2] Aging is the primary risk factor for most major causes of death in the United States, including neurodegenerative diseases and chronic inflammatory conditions.[3] Though this is a natural process that every human being will experience, the impact of aging on the body can greatly decrease quality of life. Aging is characterized by a general physiological function decline with many underlying molecular causes, including cellular senescence and genetic change and instability **(Fig. 1A)**.[4,5] Understanding the underlying processes that drive aging is vital in our effort to impact both lifespan and quality of life through the successful treatment of age-related disease.

When discussing aging research, it is important to distinguish between lifespan and healthspan. Lifespan, or life expectancy, increased by over 30 years in the United States throughout the 20th century.[6] Initially, efforts to combat causes of death in younger populations such as infectious disease and high infant mortality rates allowed more people to reach old age, followed closely by a medical shift toward targeting age-related disease. [6] Healthspan, however, is often more challenging to define, as it does not always positively correlate with lifespan and is often subjective.[6] Healthspan loosely refers to the time an

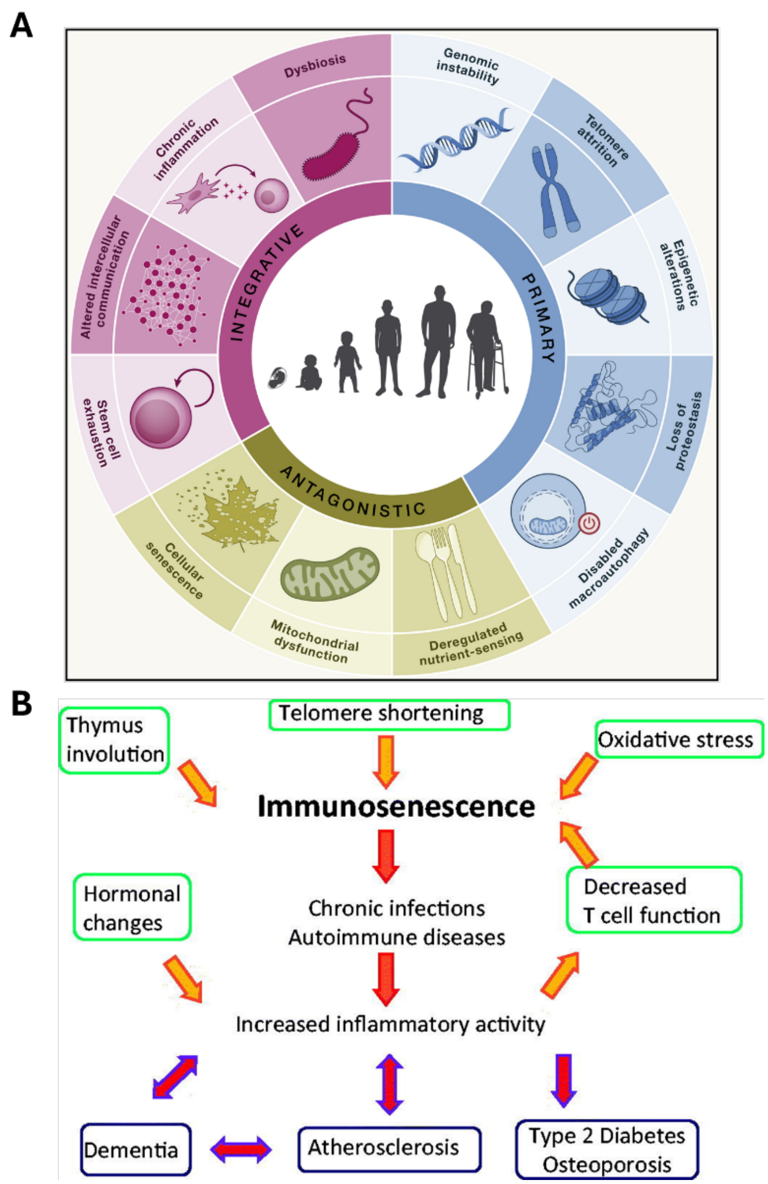

Figure 1. Overview of aging.
(A) A schematic summary of the nine hallmarks of aging. Image credit: López-Otín et. al., 2023. **(B)** Interactions between aging physiology and immunosenescence. Image credit: Castelo-Branco & Soveral, 2013

individual spends in "good" health.[7] Though health declines with age, healthspan as metric of an individual's relative health over the course of their life cannot necessarily be directly compared to their lifespan. Longevity and healthspan are often correlated, but an increase in lifespan does not always equate to increased healthspan. Additionally, "good" health is relatively subjective. Many studies evaluate healthspan, but a precise definition of what should be measured is not shared across studies. This subjectivity makes outcomes difficult to meaningfully compare between studies and highlights a need for more precise definitions and standardization within aging research. Simply increasing the number of years someone is living does not necessarily improve their overall health.[6] To optimally improve quality of life for older adults, aging studies should ideally target mechanisms to improve health, both physiological and environmental.

López-Otín et. al. originally identified 9 hallmarks of aging in a review article in 2013, and have more recently expanded this list to include 3 additional hallmarks in 2023 **(Fig. 1A)**.[4,5] Each hallmark is identified as a molecular or cellular contributor to the aging phenotype.[4] To be considered its own distinct hallmark, a process must be characterized a change that appears with age and can be experimentally altered to impact lifespan, either positively or negatively.[5] However, these processes do not act in isolation, and decline in one area may impact function in another.

Of specific interest to this project are processes contributing to age-associated immune decline. Many hallmarks identified in López-Otín et. al. contribute to or trigger cellular changes associated with immune decline. Stem cell exhaustion reduces the population of immune cells, such those involved in autophagy.[5] Cellular senescence results in increased secretion of pro-inflammatory cytokines and chronic inflammation.[8] Chronic inflammation is a newly-identified hallmark of aging that refers to the constant low-grade inflammation in the body that develops with age and contributes to the aging immune system. Though inflammation is ordinarily a beneficial innate immune response, the chronic low-level inflammation seen in older adults can lead to tissue degeneration and become pathogenic.[8] Many hallmarks of aging therefore lead to dysregulation of the innate immune response. This age-associated immune decline is often referred to as immunosenescence **(Fig. 1B)**.[9] Lessened immunity impacts healthspan, and in severe cases may decrease life expectancy. In either case, quality of life decreases dramatically. Therefore, age-associated immune decline is a clear target to improve quality of life in older adults as well as potentially increase lifespan.

II. Caenorhabditis elegans are a useful model for aging and innate immunity.

Caenorhabditis elegans are a useful model organism for both aging and genetic research. Adults are ~1 mm long and have a short total lifespan of approximately 3 weeks, making them both relatively simple to maintain in large populations and to perform efficient lifespan studies.[10] Genetically, though *C. elegans* are phenotypically distinct from mammals, they share approximately 83% of protein-coding genes with humans and therefore many conserved molecular drivers of aging, making them a suitable and useful genetic model for human disease as well as molecular aging.[11] In addition to a well-characterized genome, RNA interference is as simple as feeding worms *E. coli* expressing a double-stranded RNA (dsRNA) targeting a worm gene of interest.[12,1] Genome-wide RNAi feeding libraries for *C. elegans* are available to utilize the target gene strain without additional bacterial transformation in the lab. *C. elegans* have a transparent body structure, allowing for easy visualization of both internal tissues, dyes, and transgenically expressed fluorescent markers.[13]

C. elegans have also proven to be an effective tool in studying immune function. Though lacking an adaptive immune response, worms have an innate immune response that can provide insight into more complex pathogen-host interactions.[14] In particular, *C. elegans* are well-suited for studies of bacterial pathogenicity and anti-microbial activity. The typical worm food is a lawn of *E. coli* on an agar plate, and worms come in contact with a host of bacterial pathogens in nature. As nematodes and bacteria have evolved in close proximity, not all bacteria are pathogenic to worms.[14] Bacteria may become pathogenic through gut colonization. However, gut colonization alone does not indicate pathogenicity in worms, but rather the production of virulence factors by colonizing bacteria.[14] Many of these pathogenic bacteria in worms are also pathogenic in humans, such as the gram-positive *Pseudomonas aeruginosa* strain PA14.[14] Additionally, worms share innate immune signaling pathways with mammalian systems. Of note, *daf-16* (FOXO), *pmk-1* (p38 MAPK), and *dbl-1* (TGF-β) are all activated in immune responses in both worms and mammals.[15–17] This similarity to mammalian infection and innate immune response makes worms an apt tool to study bacterial infection and pathogenicity. However, we are not able to study adaptive immune function in worms, so testing our findings in a mammalian system is necessary to determine the role of adaptive immunity in infection.

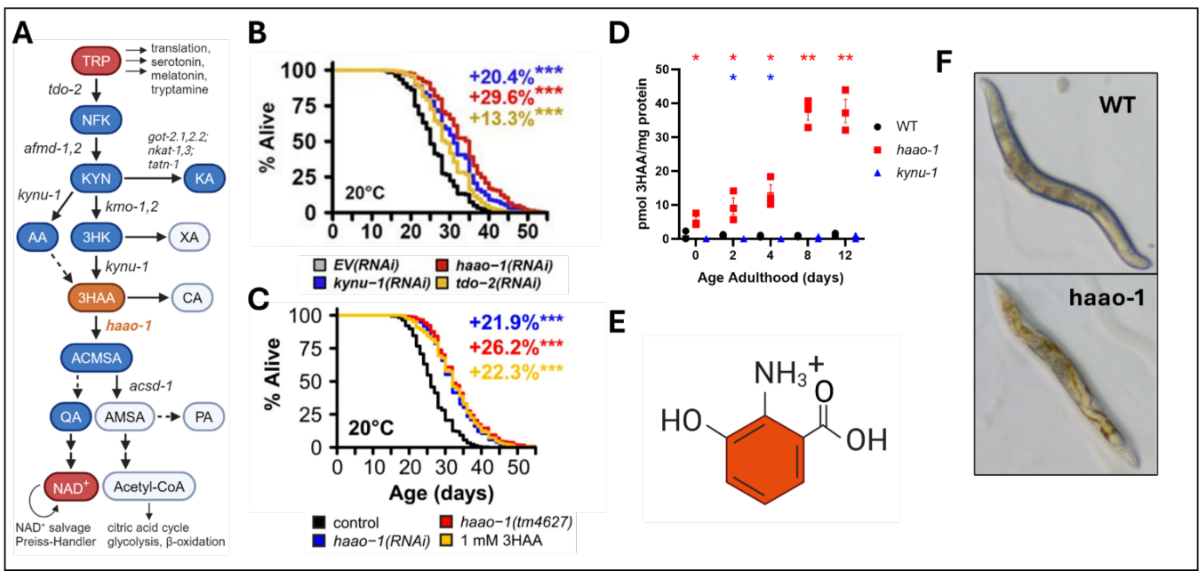

Figure 2. Summary of the kynurenine pathway and 3HAA.
(A) NAD+ synthesis via tryptophan metabolism. *kynu-1* is responsible for 3HAA synthesis, while *haao-1* regulates 3HAA degradation. Image credit: Dang et. al., 2023. **(B)** Kaplan-Meier survival curve of kynurenine RNAi worms at 20°C. *kynu-1, haao-1,* and *tdo-2* RNAi all exhibit significant lifespan extension compared to wild type (WT). *haao-1* knockdown shows the largest increase in lifespan. Image credit: Dang et. al., 2023. **(C)** Kaplan-Meier survival curve of *haao-1* knockdown and WT worms with 3HAA supplementation at 20°C. 3HAA supplementation extends lifespan similarly to *haao-1* mutation. Image credit: Dang et. al., 2023. **(D)** Mass spectrometry data of 3HAA in aging kynurenine mutant worms compared to WT. Image credit: Espejo et. al., 2024. **(E)** The chemical structure of 3HAA. **(F)** WT and *haao-1* mutant phenotype. 3HAA becomes visibly red in the *haao-1* mutant adult. Image credit: Espejo et. al., 2024.

III. Targeting the kynurenine pathway and 3-hydroxyanthranilic acid in aging.

The kynurenine pathway, the primary tryptophan metabolic pathway, has become a target in aging research. Dysfunctional kynurenine pathway activity occurs with age and has been implicated in a variety of age-related diseases, including neurodegenerative diseases like Alzheimer's and Parkinson's disease as well as cancer and cardiovascular disease.[1,18] This highly conserved pathway is responsible for ~90% of tryptophan degradation and results in the *de novo* production of nicotinamide adenine dinucleotide (NAD+) **(Fig. 2A)**.[19,20] Interventions of kynurenine pathway genes and metabolites have been shown to extend lifespan. The enzymes IDO1 (indoleamine 2,3-dioxygenase) and TDO2 (tryptophan 2,3-dioxygenase) catalyze the conversion of tryptophan to N-formylkynurenine (NFK) in humans, whereas worms rely solely on TDO2.[1] Oxenkrug et. al. first observed kynurenine pathway-mediated lifespan extension in *Drosophila melanogaster*.[21] The *vermillion* mutant is deficient in fly TDO2 and exhibits lifespan extension compared to wild type flies.[21] They later show that flies treated with a TDO2 inhibitor are also long-lived.[22] Similarly, *tdo-2* (the worm TDO2 ortholog) knockout extends lifespan in *C. elegans*.[23] Sutphin et. al. shows that knockdown of *kynu-1*, which encodes the enzyme KYNU and is responsible for the production of 3HAA, significantly extends worm lifespan.[24] Finally, Katsyuba et. al. describes that *ascd-1* knockdown extends lifespan in worms. However, both *tdo-2* and *kynu-1* knockdown result in decreased NAD+ production, while *ascd-1* knockdown promotes NAD+ production.[21,24,25]

Previous research in the Sutphin lab shows a marked increase in lifespan when the kynurenine pathway gene *haao-1* is knocked down worms by ~30% compared to wild type, a greater increase than results from knockdown of either *tdo-2* or *kynu-1* **(Fig. 2B)**.[26] *haao-1* encodes the HAAO enzyme, which is responsible for the degradation of the tryptophan metabolite 3HAA (**Fig. 1A**). With diminished or depleted HAAO function, 3HAA accumulates in the worms. Supplementing with 3HAA is sufficient to extend lifespan to a similar degree as *haao-1* knockdown and does not further extend lifespan of *haao-1* knockout worms, suggesting that 3HAA accumulation is the mediating molecular event **(Fig. 2C)**.[1] Additionally, 3HAA has an inherent red color that is easily seen in *haao-1* mutant *C. elegans* under a dissection microscope **(Fig. 2F).**[27] However, the mechanism(s) through which 3HAA acts to extend lifespan have yet to be fully determined. In this thesis I examine the working model that 3HAA increases lifespan, at least in part, by improving immune function in aging worms, thereby enhancing response to bacterial infection.

A. 3HAA plays a role in immune function in C. elegans.

In order to determine the impact 3HAA has on immune function, we first examined worm pathogen resistance in young and older adult worms. We challenged worms with the pathogenic bacterial strain PA14 at the last larval stage of development (L4), as well as days 2, 4, and 8 of adulthood **(Fig. 3A-D)**. We see the most significant lifespan extension in *haao-1* knockout worms compared to wild type when worms are infected with PA14 at day 8 of adulthood **(Fig. 3D)**. Interestingly, the red coloration from 3HAA accumulation appears around day 8 of adulthood as well.[27] However, *haao-1* knockouts still exhibit reduced pathogen tolerance as they age. *haao-1* knockout worms infected with PA14 at day 12 of adulthood show a 50% median decrease in lifespan compared to *haao-1* knockouts infected at the L4 stage **(Fig. 3E)**. Though *haao-1* mutants demonstrate an age-dependent decline in pathogen resistance, they are better able to tolerate infection at day 8 of adulthood compared to wild type worms infected at the same age. We hypothesize that the accumulation of 3HAA at this age in *haao-1* mutants may be responsible for this increase in pathogen resistance.

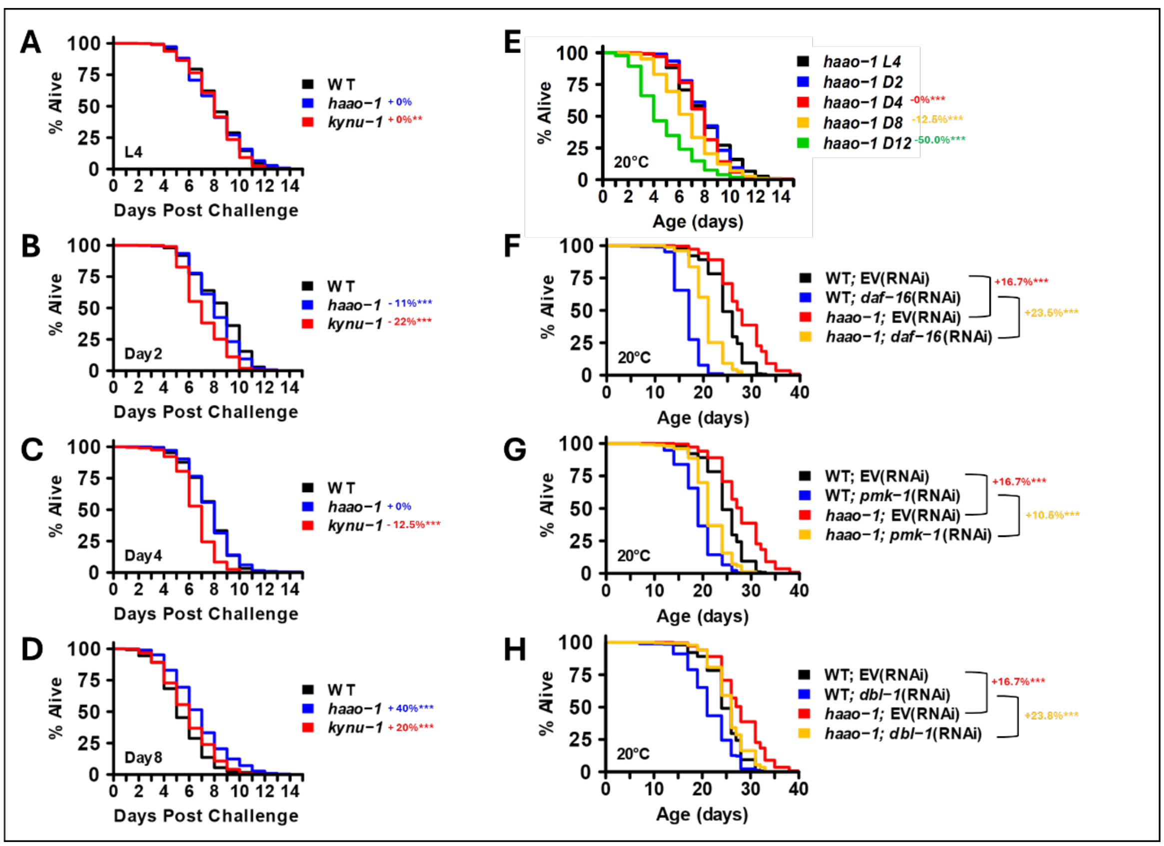

Figure 3. Kaplan-Meier survival curves of immune-challenged worms.
(A) Survival of *haao-1* & *kynu-1* RNAi worms challenged with PA14 at the L4 stage of development. **(B-D)** Survival of *haao-1* & *kynu-1* RNAi worms challenged at day 2 **(B)**, day 4 **(C)**, and day 8 **(D)** of adulthood. Accumulation of 3HAA in *haao-1* mutants at day 8 of adulthood provides improved pathogen resistance compared to wild type (WT). **(E)** Survival of *haao-1* knockout worms challenged with PA14 at days 2, 4, 8, & 12 of adulthood. Immune challenge reduces *haao-1* knockout lifespan with age compared to L4. **(F-H)** Survival of *daf-16*, *pmk-1,* & *dbl-1* immune pathway RNAi worms, respectively. *haao-1* knockout extends lifespan compared to of *daf-16*, *pmk-1,* & *dbl-1* RNAi worms. However, immune knockdown worms are short-lived compared to WT.
Percentages indicate median % change in lifespan. * p<0.05, ** p<0.005, *** p<0.0005 . All image credits: Espejo et. al., 2024.

Next, we aimed to identify a mechanism through which 3HAA accumulation in *haao-1* mutants acts to increase pathogen resistance. Worms have several established innate immune signaling pathways. Therefore, we chose to determine if 3HAA may be acting through one of these pathways to increase pathogen resistance and ultimately extend lifespan. Inactivation of *daf-16,* the worm FOXO ortholog, decreases immune response in worms.[28] Gene expression studies have shown that activation of *daf-16* results in the expression of anti-microbial peptides that aid in pathogen resistance.[28] Similarly, a worm p38 MAPK kinase, *pmk-1* also plays a role in pathogen defense. *pmk-1* is phosphorylated and activated in response to infection.[28] Lastly, the TGF-β ortholog *dbl-1* activates a pathway of small molecule signal transducers that are essential to worm pathogen resistance. Alteration of any of these pathway components lessens infection tolerance.[28] Worms on *daf-16, pmk-1,* and *dbl-1* RNAi all show a decrease in lifespan compared to wild type. In *haao-1*/immune pathway RNAi, *haao-1* knockout increases lifespan relative to wild type animals to a similar degree with or without RNAi knockdown of each immune gene **(Fig. 3F-H)**. Therefore, the *haao-1* mediated lifespan extension is likely not due to interaction of 3HAA with these established innate immune pathways. We see lifespan extension with *haao-1* knockout in both wild type and immune RNAi worms. We hypothesize that 3HAA then acts directly on the pathogen to increase resistance and extend lifespan.

B. Lysosome-related organelles in the worm gut participate in stress responses and small molecule storage.

Gut granules are lysosome-related organelles (LROs) found in the worm intestine. Though a relatively new area of research, these organelles have been shown to have a multitude of functions. As they are lysosome-related, they share some characteristics of typical lysosomes including an acidic nature and lytic enzymes.[29,30] Additionally, gut granules have an inherent blue autofluorescence as a result of the presence of anthranilic acid (AA), a 3HAA precursor in the kynurenine pathway.[31] The average gut granule fluorescence in a total worm population increases steadily as they age, but individual worm fluorescent analysis shows that fluorescence peaks just before death.[31]

The formation and development of *C. elegans* gut granules are fairly well characterized by the GLO (gut granule loss) family of genes. *glo-1* promotes GTPase activity and *glo-1* mutants have been shown to lack properly formed gut granules.[30] Orthologous to Rab32 in humans, *glo-1* loss of function worms do not exhibit the characteristic autofluorescence in the gut granules, indicative of the dysfunction in granule formation.[30] AA is unable to accumulate in *glo-1* mutants, resulting in a lack of fluorescence. While *glo-1* functions as a GTPase in gut granule formation, *glo-3* acts as a guanine exchange factor (GEF) for *glo-1* and facilitates the association of GLO-1 with the granule membrane, interrupting granule formation.[30] However, as *glo-3* is not the sole GEF for *glo-1*, we observe a phenotype with less autofluorescent gut granules than wild type in mutants, though some gut granules still form.[30] This observation implies that *glo-3* is necessary for membrane trafficking and accumulation of AA and other essential metabolites in the gut granules, as well as granule development .[30] Therefore, previous research shows that gut granule formation and maintenance are both crucial for proper LRO function.

One function that distinguishes gut granules from lysosomes is their role in zinc storage in the intestine. Using fluorescent quantification, researchers have shown that *glo-1* and *glo-3* mutant worms exhibit significantly lower zinc concentrations in gut granules than wild type, consistent with the data surrounding gut granule formation and maintenance.[32] There are two major gene families associated with zinc regulation: cation diffusion facilitators (CDFs) and Zrt-, Irt-like proteins (ZIPs). In worms, *cdf-2* localizes to gut granules and facilitates the storage of zinc as an importer[32], whereas *zipt-2.3* regulates zinc export from the gut granules in response to low cellular zinc levels.[33] Gut granules appear to be essential form normal zinc homeostasis in worms.

Interestingly, gut granules have also been implicated in responses to various types of stress. Previous researchers utilized volatile benzaldehyde (BA) to mimic an aged phenotype in young worms. Hajdú et. al. shows that at high doses, day 1 adult worms treated with BA for 4 hours show similar autofluorescence to older worms. Induction of stress via BA or *Pseudomonas aeruginosa* (PA14) resulted in activation of *daf-16* and *pmk-1*, both notable stress response and immune pathways in worms.[30] In addition to upregulation of stress response genes, researchers observed an increase in autofluorescent material in gut granules in response to BA or similar stressors, indicating an increase in lysosomal function in response to stress.[30] These experiments indicate a role for *glo-1* in activation of stress response pathways. *glo-1* and another gut granule marker, *pgp-2,* were both found to be necessary in the expression of stress response genes in response to PA14 infection.[30] The necessity of these gut granule genes in the infection response indicates a role for LROs in worm immune function in the intestine.

C. 3HAA localizes to lysosome-related organelles in the worm intestine.

Previous research in the Sutphin lab shows that 3HAA, a downstream product of *kynu-1* and AA, localizes to organelles in the gut suspected to be gut granules.[27] Though these organelles morphologically resemble LROs, we have yet to definitely identify them as such. Additionally, 3HAA is synthesized in the hypodermis and is degraded in the neurons, meaning it is not synthesized or degraded in the gut **(Fig. 4A)**. Additionally, we see that bacteria also localizes to gut granules, which are an acidic zinc-rich environment **(Fig. 4B)**. Lysosomes are known to be a bacterial degradation site in cells. As a part of autophagy, bacteria are engulfed in phagolysosomes, a fusion of a phagosome and lysosome in response to infection.[34] Pathogens have evolved ways to avoid degradation in the cell, including mechanisms to avoid recognition by the immune system and prevention of phagosome formation.[35] Worm LROs do retain some lysosome-like functions due to their acidity and the presence of hydrolases.[30] This may be the cause of bacterial localization to these organelles. Additionally, we have shown that 3HAA incurs some pathogen resistance in worms to extend lifespan. We see a distinct green coloration in PA14 infected LROs, as well as in increase in red 3HAA in the same location in response to infection **(Fig. 4B)**.[27] We therefore hypothesize that 3HAA's pathogen resistance in worms may take place at the gut granule. Additionally, we seek to explore the role of stored zinc within the granules as a part of this immune impact.

IV. Thesis Overview

Throughout this project, I chose to examine two questions that arise from earlier work on the localization of 3HAA and its role in pathogen resistance.[27] First, I investigate the mechanisms of 3HAA transport within the worm intestine. Second, I aim to characterize the interaction between 3HAA, bacterial pathogens, and zinc to understand the impact of 3HAA on bacterial pathogens. I hypothesize that 3HAA improves pathogen resistance in worms by killing or inhibiting bacterial growth in the gut granules. Additionally, I explored the role of zinc in both pathogen resistance as well as 3HAA transport due to its localization within the granules.

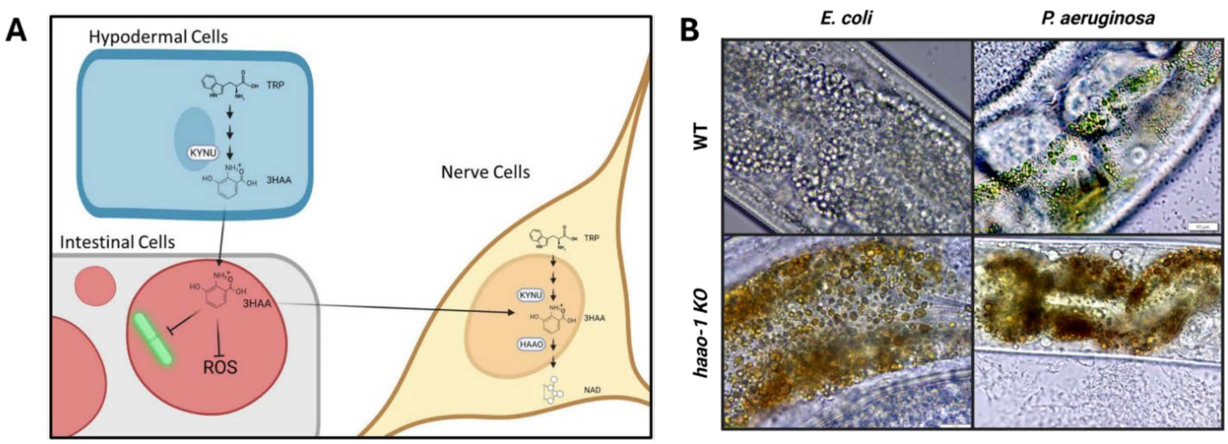

Figure 4. Thesis Overview
(A) 3HAA is synthesized by KYNU in the worm hypodermis, travels to the gut granules in the intestine, then ultimately transports to the neurons where it is degraded by HAAO. Our working model is that 3HAA may serve an immune function in the granules. **(B)** Microscopy images of wild type (WT) and *haao-1* knockout worms infected with *E. coli* or *P. aeruginosa.* Images taken just below the pharyngeal pump. Image Credits: Espejo et. al., 2024.

RESULTS

I. 3HAA Transport and Localization

The transport mechanism of 3HAA within the gut has yet to be identified. In order to elucidate this mechanism, I systematically knocked down target genes in worms involved in molecular pathways or processes implicated in small molecule trafficking using RNA interference (RNAi). I selected genes to screen based off of both the chemical structure of 3HAA as well as the lysosome-like function of gut granules. Amino acids consist of an amino group (NH2), a carboxyl group (COOH), and a variable R group. Given 3HAA's structural similarity to this amino acid structure, particularly tyrosine with a hydroxyl R group, we first chose to target amino acid transporters as a potential mechanism of 3HAA transport **(Fig. 2E)**. Additionally, 3HAA is a metabolite of tryptophan, another amino acid.[1] However, none of our target genes visibly impacted the tell-tale red phenotype compared to *haao-1* knockout worms fed empty vector bacteria. Therefore, we shifted our focus to genes involved in lysosomal formation and stability. Given our hypothesis that 3HAA is localizing to LROs specifically, targeting genes that impact lysosome or LRO formation similar to *glo-1* or *glo-3* will inhibit 3HAA localization. However, while interrupting gut granule structure and function will illustrate how 3HAA enters the granules, it does not give us much insight as to how it travels to the gut granules. Therefore, we simultaneously explored vesicular trafficking as a potential mechanism of action.

A. 3HAA produces a distinct phenotype in haao-1 knockouts.

To investigate the impact of each target gene on 3HAA transport, I performed a qualitative RNAi screen using *haao-1* worms. A full list of target genes and their reported functions can be found in Supp. Table 1. I fed *haao-1* knockout worms *E. coli* bacteria (strain HT115) bacteria targeting amino acid transport, lysosome formation, and vesicular transport. 3HAA is naturally a vibrant red in color and therefore quite easy to see in the translucent worm under a stereo microscope. For roughly two weeks, I observed worms daily to note any significant visual changes in red coloration between the *haao-1* knockout control and RNAi strains. I chose to image the gut granules in each worm strain at day 8 of adulthood as this is when *haao-1* control worms are visibly red yet still healthy, as gut granules become less stable and break down with age. Under 100x magnification, 3HAA's red coloration becomes more clearly visible within the LROs specifically. For consistency, we took two images per strain where gut granules tend to congregate: just under the grinder and next to the vulva. Additionally, I explored the impact of a selection of these target genes on worm lifespan. I hypothesize that if 3HAA is not able to properly localize to the granules with bacteria, pathogen resistance will be diminished and therefore lifespan will be reduced in RNAi worms.

B. Lysosome formation and vesicular transport gene knockdown disrupts 3HAA localization to LROs.

lyst-1

Lyst-1 is a BEACH (Beige and Chediak-Higashi) domain containing protein (BDCP) necessary for gut granule biogenesis.[36,37] BDCPs all share a highly conserved BEACH domain in eukaryotes, but variability in the remaining protein structure denotes specific cellular function. Currently identified BDCPs are known to impact cell signaling, membrane dynamics, immune function, and epigenetic modifications.[36] Mutations in the *lyst-1* gene disrupts gut granule formation specifically, resulting in smaller fragmented granules.[36] We found that RNAi knockdown of *lyst-1* in *haao-1* knockout animals produces visibly less accumulation of 3HAA in the gut granules compared to *haao-1* knockout worms on empty vector RNAi **(Fig. 5C)**. Though we did not see the dramatic decrease in gut granule size seen in *lyst-1* knockout worms, RNAi knockdown impeded *lyst-1* function sufficiently to disrupt 3HAA localization to the gut granules typically seen in *haao-1* knockout worms. Interestingly, while *haao-1* knockout extends lifespan in *lyst-1* RNAi (~22%), *haao-1* knockout extends lifespan to a greater degree in empty vector controls (~30%) **(Fig. 6A)**. Given this similarity in *haao-1* lifespan extension in *lyst-1* knockdown and wild type, *lyst-1* knockdown does not appear to have a dramatic impact on worm lifespan.

uso-1 and syx-7 – the SNARE complex

uso-1, the worm P115 ortholog, is a soluble N-ethylmaleimide-sensitive factor attachment protein receptor (SNARE) tethering factor involved in vesicular transport from the endoplasmic reticulum (ER) to the Golgi.[38] The docking of vesicles to their target membranes in intracellular vesicular transport requires a multitude of specific proteins. The vital components of the SNARE complex are an N-ethylmaleimide-sensitive factor (NSF), an ATPase, and a soluble NSF-attachment protein (SNAP).[39] Additional proteins denote specificity to a particular target membrane and aid in docking, including syntaxins and tethering factors.[39]

Previous research by Gkikas et. al. noted that *uso-1* often localizes to the mitochondria and may have a role in autophagy regulation. Though the SNARE complex is most often associated with synaptic signaling of neurotransmitters in the neurons, we found that *uso-1* knockdown in a *haao-1* knockout worm results in lessened 3HAA accumulation in the gut granules **(Fig. 5D)**. Additionally, I found that *uso-1* RNAi reduces lifespan by ~17% in wild type worms **(Fig. 6B)**. However, *haao-1* knockout extends mean lifespan in *uso-1* knockdown worms by 31%. Comparatively, *haao-1* knockout in empty vector control worms extends mean lifespan by only 13% **(Fig. 6B)**. Therefore, *haao-1* knockout appears to extend lifespan to a greater degree in the absence of *uso-1* than in wild type worms.

Syx-7 is the worm ortholog of human syntaxins 7 and 12 and serves as part of the SNARE complex in vesicle trafficking.[40] Syntaxins are transmembrane proteins that also aid in the docking of vesicles to their target membranes during transport.[39] We found that *syx-1* knockdown in *haao-1* knockout worms also disrupted 3HAA transport; RNAi worms showed less red 3HAA accumulation in the gut granules **(Fig. 5E)**.

zipt-2.3

As previously stated, a key role of the gut granule is zinc homeostasis. *Zipt-2.3* is transcribed in response to low cellular zinc levels and releases zinc stored in the gut granule.[33] Curiously, when *zipt-2.3* is depleted, *haao-1* knockouts show a disruption in 3HAA localization to the gut granule. *haao-1* knockouts on *zipt-2.3* RNAi were noticeably less red in color than *haao-1* knockout controls **(Fig. 5F)**. Additionally, LROs in these knockdown worms appear much older than the age of worm as indicated by the increase in green coloration. I have observed that in older adult worms, LROs appear particularly green or blue. Aging gut granules also experience an increase in blue fluorescence before death.[31] Though I have not confirmed that *zipt-2.3* RNAi induces this death fluorescence, it appears that this change in color is somewhat indicative of intestinal health in worms. Therefore, in addition to a disruption of 3HAA localization, *zipt-2.3* knockdown gives gut granules a more aged phenotype.

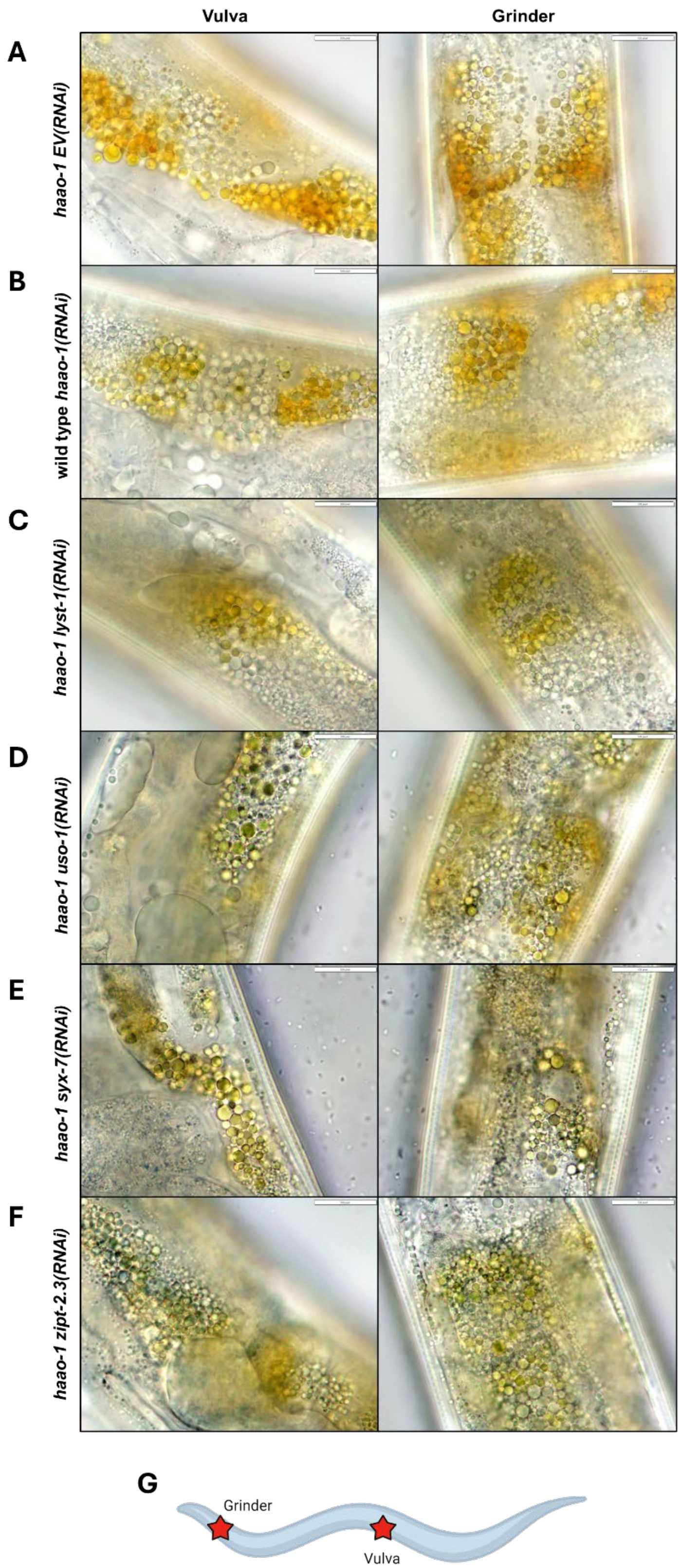

Figure 5. Confocal microscopy images of 3HAA localization to the gut granules at day 8 of adulthood in haao-1 RNAi worms. Left images taken adjacent to the vulva, right images taken just under the grinder. **(A)** *haao-1* knockout worms on *EV(RNAi)*. Typical 3HAA accumulation in *haao-1* knockout worms. **(B)** wild type worms on *haao-1(RNAi).* Similar 3HAA accumulation as *haao-1 EV(RNAi)* controls. **(C-F)** *haao-1* knockout worms on *lyst-1(RNAi)* **(C)**, *uso-1(RNAi)* **(D)**, *syx-7(RNAi)* **(E)**, and *zipt-2.3(RNAi)* **(F)**. All show a less vibrant red 3HAA accumulation as compared to *haao-1 EV(RNAi)* control. **(G)** Schematic of worm image locations.

II. 3HAA has an antibiotic function.

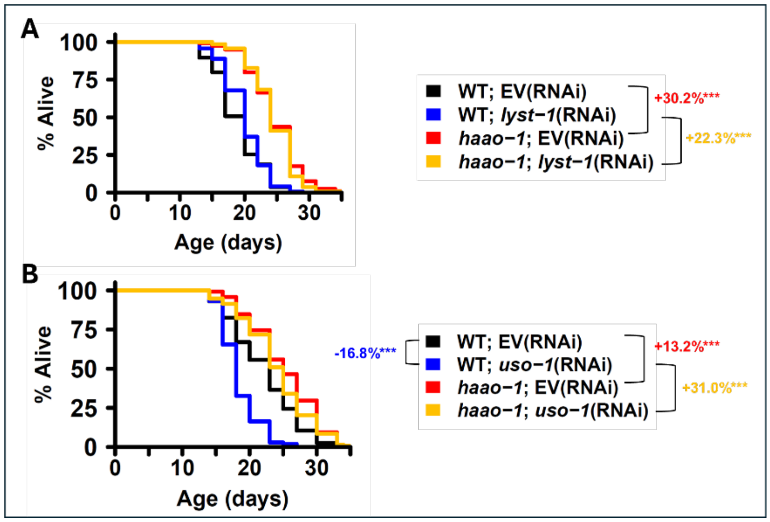

Figure 6. Kaplan-Meier survival curves of wild type (WT) and haao-1 knockout worms with RNAi knockdown of lyst-1 & uso-1. Comparisons without mean percentages shown are not significant. * $p<0.05$, ** $p<0.005$, *** $p<0.0005$.
(A) *lyst-1(RNAi)* does not significantly affect worm lifespan from WT. *haao-1* knockout extends lifespan in *lyst-1(RNAi)* less than *haao-1* knockout alone. **(B)** *uso-1(RNAi)* decreases lifespan from WT. However, *haao-1* knockout in *uso-1(RNAi)* worms increases lifespan.

haao-1 mutants accumulate 3HAA and exhibit lifespan extension under both normal and immune-challenged conditions (**Fig. 3, 4**).[27] Therefore, we hypothesize that this excess 3HAA provides some additional immune protection contributing to the observed lifespan extension. However, *haao-1* knockout extends lifespan in both immune deficient and wild type worms, indicating the potential role for 3HAA does not act through established worm innate immune pathways **(Fig. 3F-H)**.[27] Additionally, we see an accumulation of bacterial pathogens in LROs localized with 3HAA in the worm intestine, suggesting that 3HAA interacts with pathogens directly in the gut to illicit resistance **(Fig. 4B)**. I thus chose to explore 3HAA's impact on pathogenicity. To that end, I measured bacterial growth in liquid culture to determine the impact of 3HAA treatment on *E. coli ex vivo*. I hypothesize that 3HAA impedes bacterial growth and therefore reduces pathogenicity, resulting in increased pathogen resistance *in vivo.*

The bacteria growth curve is sigmoidal and defined by several distinct phases **(Fig. 7A)**.[41] We focused here on measuring the max velocity of the culture as well as the time spent in the lag phase, referred to as lag time.[41] Max velocity (Vmax) is a measurement of the fastest growth rate reached during the log phase, or the exponential phase, and can be determined by the greatest slope on the growth curve (**Fig. 7A)**. These two metrics provide different ways to measure the impact of 3HAA and zinc sulfate treatment in *Escherichia coli*. Bacteria culture density was measured and diluted as a normalization step such that each 250 µl well started at an optical density of 0.1 at 600 nm to standardize the starting bacteria population **(Fig. 7B)**.

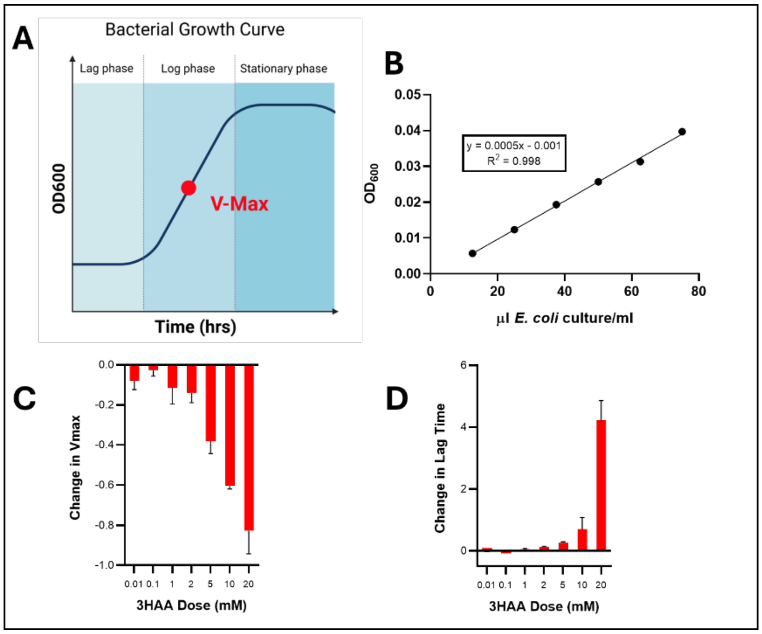

Figure 7. 3HAA as an antibiotic.
(A) A diagram of an idealized bacterial growth curve in liquid culture. Vmax indicates maximum slope of the optical density curve in the log phase. Lag time indicates time spent in the lag phase. Image credit: Espejo et. al., 2024. **(B)** Sample OD600 linear regression for cell number normalization in culture. Linear regression of OD600 readings for serial dilutions of *E. coli* culture is used to estimate OD600 0.1 in wells. **(C-D)** Change in max velocity **(C)** and change in lag time **(D)** of *E. coli* treated with increasing 3HAA doses for 24 hours. 3HAA reduces Vmax and increases lag time in a dose-dependent manner.

A. 3HAA inhibits E. coli growth.

We performed a series of liquid bacterial growth assays measuring optical density over time to determine the impact of 3HAA on two metrics of bacterial growth. As worms are typically fed a lawn of *E. coli*, we measure the growth of a fluorescent strain of *E. coli* developed in the lab. The addition of GFP does not have a significant impact on growth and is otherwise identical to the typical *E. coli* strain. This fluorescent strain is utilized for other concurrent immune function studies in the lab and was therefore chosen for consistency. We assayed seven doses of 3HAA from 0.01 to 20 mM over 24 hours. We found that 3HAA treatment has a dose-dependent impact on both max velocity and lag time at doses of 1 mM or higher. As 3HAA dose increases, max velocity decreases and lag time increases compared to untreated *E. coli* **(Fig. 7C-D)**.

B. Supplemental zinc enhances 3HAA's antibiotic effect.

Zinc homeostasis is vital not only for host organism health, but for pathogens as well. We previously established that gut granules are a storage site for intestinal zinc, and 3HAA localizes to the granules.[32] Additionally, RNAi knockdown of the major gut granule exporter *zipt-2.3* results in less 3HAA accumulation within the granules **(Fig. 5F)**. Given this colocalization and potential interaction, I aimed to determine the effect of supplemental zinc and 3HAA on bacterial growth. First, I measured zinc's effect on *E.coli* growth without concurrent 3HAA treatment. I chose concentrations of zinc sulfate from 0.2 mM to 1 mM, as preliminary zinc dose responses in *E. coli* show a plateau in the effect on Vmax at around 2 mM **(Supp. Fig. 1A)**. We see that, similar to 3HAA, zinc treatment impedes *E. coli* growth in a dose-dependent manner; Vmax decreases and lag time increases as zinc concentration increases **(Fig. 8A-B)**.

Next, we combined our zinc doses with 1 mM 3HAA, as this concentration significantly slows bacteria growth without being toxic on its own. With the addition of 3HAA to the previous zinc concentrations, we see ~2-fold decrease in max velocity compared to the respective zinc concentrations alone **(Fig. 8E)**. We also see a dramatic increase in lag time **(Fig. 8F)**. Both observed effects remain dose dependent.

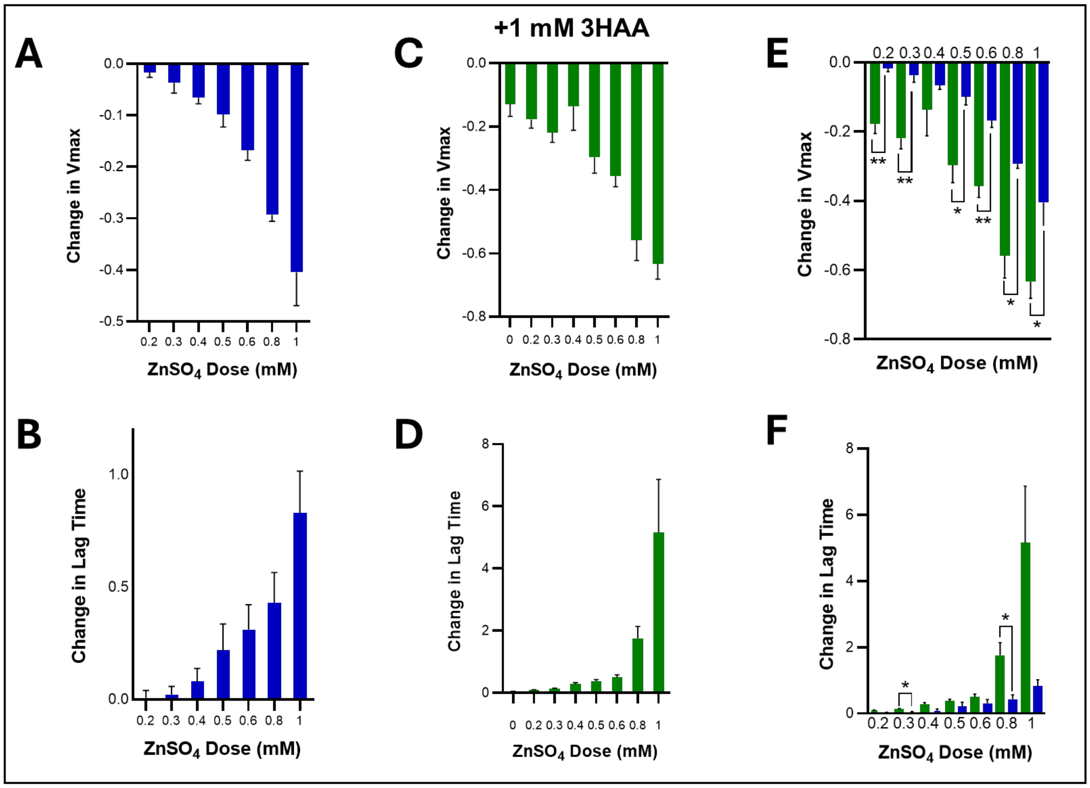

Figure 8. Impact of 3HAA and zinc treatment on *E. coli* growth in liquid culture.
(A-B) Change in max velocity **(A)** and lag time **(B)** in *E. coli* treated with increasing doses of zinc sulfate for 24 hours*. Zinc treatment decreases Vmax and increases lag time in a dose-dependent manner. **(C-D)** Change in max velocity **(C)** and lag time **(D)** in *E. coli* treated with increasing zinc doses with 1 mM 3HAA. **(E)** Combination of (A) and (C) for comparison. All zinc sulfate doses apart from 0.4 mM show a significant decrease in Vmax with the addition of 1 mM 3HAA. **(F)** Combination of (B) and (D) for comparison. 0.3 mM & 0.8 mM zinc sulfate show a significant increase in lag time with the addition of 1 mM 3HAA.
Data represents 3 biological replicates per treatment. All conditions normalized to untreated *E. coli* control. Zinc sulfate doses in blue, zinc sulfate doses with 1 mM 3HAA treatment in green. Unpaired t-tests used to determine significance in (E-F). * $p<0.05$, ** $p<0.01$, *** $p<0.001$.
*One biological replicate contaminated after 8 hours. Data after 8 hours was disregarded for that replicate.

DISCUSSION & CONCLUSIONS

In the absence of HAAO, the metabolite 3HAA accumulates in granule-like structures in the intestinal cells of *C. elegans* leading to longer lifespan. Though the precise mechanism through which 3HAA accomplishes this has yet to be fully described, we find that one likely mechanism is that 3HAA increases worm pathogen resistance through interaction and association in the intestine.

Our RNAi screen suggests that 3HAA is likely transported to gut granules in the worm intestine via vesicular trafficking. Though 3HAA is neither synthesized nor degraded in the gut, we find that 3HAA and infectious bacteria colocalize in gut granules. *uso-1* and *syx-7* encode SNARE complex proteins involved in vesicle docking at the target membrane; in this case, the granule membrane. RNAi targeting both SNARE genes visually disrupts 3HAA localization to gut granules **(Fig. 5D-E)**. Additionally, *haao-1* knockout extends lifespan in the absence of *uso-1* to a greater degree than in wild type worms **(Fig. 6B)**. Though this finding disagrees with the hypothesis that disruption of 3HAA transport in the gut reduces lifespan, it is intriguing. We have thus far observed 3HAA localization in LROs, but 3HAA may be present elsewhere contributing to lifespan extension; 3HAA localization to these granules may not be essential to the long-lived *haao-1* knockout phenotype. Replication of this lifespan study in order to confirm these observations is vital, as well as 3HAA quantification in the gut. Analyzing expression patterns of these genes in the worm would also provide insight into the mechanism of 3HAA-mediated lifespan extension in these RNAi worms. Additionally, this lifespan study was performed using the HT115 RNAi *E. coli* feeding strains. However, the lab observes that *haao-1* mutant lifespan extension is more pronounced in worms fed the strain OP50, the typical worm laboratory food, than in HT115. Therefore, I would like to compare *haao-1* knockout lifespan extension in *uso-1* RNAi worms in each of these strains as well. Additionally, comparing *uso-1* RNAi lifespan to *syx-7* RNAi lifespan would be beneficial in determining the role of the SNARE complex in 3HAA trafficking. Finally, I would like to explore additional SNARE and vesicular trafficking genes in the future to confirm this method of 3HAA transport.

In addition to SNARE genes, *lyst-1* knockdown disrupts 3HAA localization in the gut **(Fig. 5C)**. As depletion of *lyst-1* results in reduction and fragmentation of gut granules, interrupting gut granule biogenesis should impede 3HAA import since granules are unable to form properly. While SNARE gene knockdown inhibits 3HAA transport via vesicle localization, *lyst-1* knockdown presumably acts upstream of this process, disrupting gut granule formation and inhibiting 3HAA from entering. Additionally, this finding supports the hypothesis that 3HAA is localizing to LROs specifically; targeting LRO formation results in reduced 3HAA accumulation. However, unlike *uso-1*, *haao-1* knockout does not appear to have an impact on *lyst-1* RNAi lifespan. Though *haao-1* knockout significantly increases lifespan in both wild type and *lyst-1* RNAi, the mean lifespan extension is similar **(Fig. 6A)**. It is possible that though 3HAA can no longer localize to the gut granules, it is still present elsewhere in the worm and therefore lifespan and relative health remains unchanged, further necessitating 3HAA quantification. We have found that 3HAA is autofluorescent, and fluorescent imaging of these RNAi strains may be beneficial in determining 3HAA localization in tissues outside of the gut. This technique has yet to be fine-tuned, as the 3HAA fluorescent emission, though in the red range, is relatively non-specific, so identifying red fluorescence as 3HAA is not completely reliable. As with analyzing SNARE gene expression in the worm, noting 3HAA accumulation in different tissues would aid in identifying a potential lifespan extension mechanism.

Previous research in the lab shows that 3HAA accumulation in *haao-1* mutants boosts pathogen resistance in worms **(Fig. 3A-D)**. However, it does not appear to act through established worm innate immune pathways as *haao-1* knockout extends lifespan in both immune pathway RNAi and wild type worms **(Fig. 3F-H)**. We have shown that 3HAA acts on pathogens directly to impede bacterial growth. 3HAA treatment both increases max velocity and decreases lag time in liquid culture, slowing overall bacterial growth. However, liquid bacterial culture differs from the gut granule environment. Further studies are necessary to confirm this interaction *in vivo.* Additionally, though a precise concentration of 3HAA in LROs has yet to be determined, the accumulation of 3HAA within the granules suggests that the concentration is higher in the organelle than in the worm as a whole. This higher concentration may be contributing to pathogen resistance in gut granules. Alternatively, 3HAA may accumulate elsewhere in the intestine, and the colocalization of 3HAA with the pathogen is the key factor in its antibiotic function, rather than the site of colocalization. We are currently working to fluorescently identify sites of 3HAA and bacteria colocalization in the gut, which would confirm whether this interaction occurs outside of LROs. In addition, I would like to explore the impact of RNAi knockdown of identified 3HAA transport genes on infection. Through a novel worm imaging method, we can fluorescently track bacterial infection in the worm gut in individual worms.[42,43] My hypothesis is that if these 3HAA transport genes reduce total 3HAA in the gut when knocked down, worms will show increased infection as a result of decreased pathogen resistance. Accompanying immune-challenged lifespan studies of these worms on PA14 would show if the hypothesized increased infection decreases lifespan.

In addition to bacteria and 3HAA colocalization, gut granules act as a zinc storage site in the worm intestine. Given the colocalization of these three elements, I explored the impact of zinc on the antibiotic effect seen with 3HAA treatment in liquid culture. I show that zinc treatment alone produces a similar trend to 3HAA treatment; as zinc concentrations increase, so does lag time **(Fig. 8B)**. Conversely, Vmax decreases with increasing zinc doses **(Fig. 8A)**. With the addition of 1 mM 3HAA to these zinc concentrations, we see an additive effect on Vmax and a synergistic effect on lag time **(Fig. 8C-D)**. Most dramatically, at the highest zinc dose measured we see ~5-fold increase in lag time with the addition of 3HAA **(Fig. 8E-F)**. These findings indicate that zinc may enhance 3HAA's antimicrobial properties, and vice versa, in the gut.

Notably, I found that RNAi knockdown of the gut granule zinc exporter *zipt-2.3* disrupts 3HAA localization to the gut granules. Given that *zipt-2.3* is transcribed in response to low cellular zinc concentrations, I hypothesize potential roles for zinc in the observed immune function as well as 3HAA transport. First, zinc may simply be toxic to pathogenic bacteria in a manner similar to but separate from 3HAA. In *zipt-2.*3 RNAi, zinc can still enter the granules, but much less can be exported. Therefore, the increase in zinc concentration within the granule may contribute to pathogen resistance in addition to the 3HAA's impact. Second, GTPase activating proteins (GAPs) have been shown to be necessary for vesicle budding from the Golgi.[44] In a study by Cukierman et. al., a GAP with a zinc-finger domain requires this domain to form vesicles. Given that 3HAA is likely trafficking to the gut granules in vesicles and *zipt-2.3* regulates zinc export, a reduction or loss of free zinc in the *zipt-2.3* RNAi worms may prevent vesicle formation through dysfunction of GAP zinc-finger domains, and therefore 3HAA transport. Exploring the immune capacity of these knockdown worms *in vivo* is vital to further understand zinc's role in both 3HAA transport and pathogen resistance.

In the future, testing these findings in a mammalian model system would be beneficial in translating potential immune benefits to humans. Similar to worms, *haao-1* knockout mice are longer lived relative to wild type mice.[1] Additionally, mice fed a diet supplemented with 3HAA exhibited similar lifespan extension.[1] As previously noted, the worm immune system differs greatly from ours. However, measurement of mouse immune cell populations in mice fed chow supplemented with 3HAA shows that B cells and natural killer (NK) cells both decrease with 3HAA treatment compared to controls.[1] The decrease in innate immune activation in response to 3HAA treatment supports its anti-inflammatory role. These findings also support the hypothesis that 3HAA has beneficial effects on immune function.

Given my findings and previous research, I would like to further explore 3HAA's role in a mammalian system in the future. Mammalian systems are inherently more complex than nematodes, and 3HAA may have more beneficial impacts on health than can be identified in worms. In a recent study, 3HAA was shown to inhibit inflammasome assembly and cytokine secretion by macrophages, contributing to its anti-inflammatory function and reducing atherosclerosis in mice.[45] In liver cancer, increased 3HAA reduces hepatocellular carcinoma (HCC) tumor growth by inducing tumor cell apoptosis.[46] Cardiovascular disease, chronic inflammation, and cancer development are all common age-related diseases, further supporting the anti-aging benefits of 3HAA.

The colocalization of 3HAA, bacteria, and zinc within the worm gut granules plays a key role in immune function and health. Though there is much more to learn about 3HAA and its role in aging, these findings show compelling evidence for 3HAA colocalization with pathogens via vesicular transport in the intestine. The complex nature of the relationship between 3HAA and zinc homeostasis in immunity leaves much to be explored in the future.

MATERIALS & METHODS

Strains. Wild type (N2) worms, *Escherichia coli* OP50 bacteria, and *E. coli* HT115 empty vector (EV) bacteria were originally obtained from Dr. Matt Kaeberlein (University of Washington, Seattle, WA, USA). Strains *kynu-1*(tm4924) X (FX04924; backcrossed 6x to N2 to create strain GLS129) and *haao-1*(tm4627) V (FX04627; backcrossed 6x to N2 to create strain GLS130) were obtained from the *C. elegans* National Bioresource Project (NBRP) at the School of Medicine at the Tokyo Women's Medical University. RNAi feeding vectors in the *E. coli* HT115 background were obtained from the Ahringer (Source Bioscience) or Vidal (Horizon Discovery Darmacon Reagents RCE1181) RNAi feeding libraries. *Pseudomonas aeruginosa* strain PA14 was used for worm immune challenge conditions.

Media and culture. We maintained worms on solid nematode growth media (NGM) seeded with *E. coli* bacteria at 20°C as previously described[47] except where otherwise noted. RNAi experiments used *E. coli* strain HT115, while bacterial growth assays used OP50 tagged with GFP (GOP50) liquid culture. Growth behavior in OP50 and GOP50 is comparable. We conducted RNAi feeding and lifespan assays according to standard protocols. All worms were transferred to NGM plates containing 50 µM 5-fluorodeoxyuridine (FUdR) starting at the L4 larval stage to prevent reproduction.

RNA interference (RNAi). All experiments were conducted on NGM containing 1 mM Isopropyl β-D-1thiogalactopyranoside (IPTG) to activate production of RNAi transcripts and 25 µg/mL carbenicillin to select RNAi plasmids and seeded with live E. coli (HT115) containing RNAi feeding plasmids. Worms were age-synchronized via timed egg laying at the experimental temperature and transferred to plates containing 50 µM 5-fluorodeoxyuridine (FUdR) to prevent reproduction at the L4 larval stage as previously described[47].

Lifespan analysis. Lifespan and paralysis experiments were conducted as previously described[47]. Briefly, adult animals were maintained on NGM RNAi plates with FUdR throughout life. Each animal was examined every 2-3 days by nose- and tail-prodding with a platinum wire pick. Animals were scored as dead if they failed to react to prodding. Live and dead animals were counted, and dead animals removed from the plate at each examination. Animals displaying vulva rupture were included in all analyses, while worms that left the surface of the plate were excluded.

Each lifespan experiment included test groups consisting of 105-150 worms (3 plates with 35-50 worms/plate). Each experiment included a negative control test group fed *E. coli* strain matched to the test conditions. For lifespan epistasis and tissue-specific RNAi experiments, each combination of candidate gene RNAi and mutant/transgenic strain was measured in three independent experiments, each including: wild type worms fed EV(RNAi), wild-type worms fed candidate RNAi, mutant worms fed EV(RNAi), and mutant worms fed candidate RNAi. P-values for statistical comparison of lifespan between test groups were calculated using the log-rank test (survdiff function in the R "survival" package) with Holm multiple test correction applied to comparisons made within each experiment. Mean lifespan percentages indicate change in average day of worm death. Median lifespan percentages indicate change in the day at which 50% of worms have died.

Liquid Culture Bacteria Growth Assays. GOP50 colonies were inoculated at least 16 hours prior to assay from a single colony and grown in a Lab-Line Incubator-Shaker at 250 RPM and 37°C. Masses of 3HAA (CAS: 548-93-6) and zinc sulfate (CAS 7446 20-0) were used to create 200 mM and 1 mM stock solutions, respectively. Serial dilutions of 3HAA and zinc sulfate were made using LB broth and stock solutions, then added to a clear 96-well tissue culture plate. OD_{600} measurements were taken of serial dilutions of GOP50 just prior to assay to ensure consistent cell populations in wells. GOP50 culture was diluted such that each individual well begins at a starting cell concentration of OD_{600} 0.1. Standardized GOP50 culture was added to wells using a p200 multichannel micropipette just before measurement. 96 well plates were placed in a microplate reader for 24 hours at 37°C. OD_{600} measurements were taken every 15 minutes with constant shaking in the meantime to prevent biofilm formation. Data was analyzed using Biotek Gen5 3.12 software and presented in GraphPad Prism 8.4.3.

High resolution microscopy.

High resolution microscopy was performed on an Olympus IX83 DSU fluorescent spinning disk confocal microscope using differential interference contrast (DIC) light. Monochrome images were captured with a ORCA-FLASH4.0LT+ sCMOS monochrome camera and color images with a DP27-CU-1-2 5MP color camera. For 40X confocal imaging, 100x confocal imaging, and 100X color imaging *C. elegans* were plated on 2.2% agarose pad mounted on a 1 mm thick slide. 25 mM levamisole was used to paralyze the animals. For confocal microscopy the animals were given 15 minutes in the levamisole before imaging in order to complete the paralysis prior to collecting z-stack images. Image deconvolution was performed using cellSens software and analyzed using Arivis 4K.

SUPPLEMENTAL FIGURES

Table 1. A complete list of the 48 candidate genes screened. Genes without cited references credited to Wormbase.

	Gene	Reported Function	Reference
Intracellular Transport			
	cup-5	endocytosis; located in the lysosome	Fares & Greenwald et. al., 2001
	rab-10	endocytosis in the intestine	Chotard et. al., 2010
	rab-2 (unc-108)	vesicular trafficking & endocytosis; GTPase	
	rab-5	vesicular trafficking & endocytosis; GTPase	
	rme-6	vesicular trafficking & endocytosis; rab-5 GAP	
	rab-7	vesicular trafficking & endocytosis; GTPase	
	rab-6.1	retrograde endocytic recycling	Zhang et. al., 2016
	skat-1	transmembrane amino acid transporter in LROs	Soukas et. al., 2013
	cav-1	required for cav-2 localization	Williams & Lisanti et. al., 2004
	cav-2	intestinal trafficking & signaling	Parker et. al., 2009
	sec-10	endocytic recycling	Chen et. al., 2014
	vps-29	retrograde intracellular trafficking	
	vps-22	vesicular trafficking	
	rabr-2	vesicular trafficking	
	did-2	vesicular trafficking	
	eas-1	Golgi vesicle trafficking	
	uso-1	vesicular trafficking; SNARE complex component	
	C31E10.6	vesicular transport	
	C34D4.4	vesicular transport	
	sftd-3	vesicular transport	
	gop-1	rab-2 activator	Yin et. al., 2017
	vps-33.1	vesicular trafficking	
	trpp-10	vesicular trafficking	
	syx-7	vesicular trafficking; SNARE complex component	
	cup-16	endocytosis; located in the lysosome	
	sel-9 (tmed-2)	vesicular trafficking	
	vps-60	vesicular trafficking	
	trpp-5	vesicular trafficking	
Organelle Biogenesis			
	vps-16	gut granule biogenesis	
	vps-41	gut granule biogenesis	
	glo-3	gut granule biogenesis	Rabbitts et. al., 2008
	lyst-1	gut granule biogenesis	
	dsbn-1	gut granule biogenesis; BLOC-1 component	
	snpn-1	gut granule biogenesis & vesicular trafficking; BLOC-1 component	
	glo-2	gut granule biogenesis; BLOC-1 component	Morris et. al., 2018
	mrp-3	gut granule biogenesis	Tan et. al., 2023
	pgp-2	gut granule biogenesis	Schroeder et. al., 2007
	mrp-4	gut granule biogenesis	Currie et. al., 2007
	cup-15	lysosome organization	
	blos-7	LRO biogenesis	
	blos-8	LRO biogenesis	
Organelle Organization			
	kxd-1	lysosomal positioning	Griffin et. al., 2019
	wht-7	intracellular localization of LROs	Brandt et. al., 2022
Zinc			
	cdf-2	intestinal zinc transporter	Davis et. al., 2009
	zipt-2.3	gut granule zinc transporter	
Immune Response			
	asp-12	pathogen defense in the lysosome	Mack et. al., 2022
	ilys-3	pharyngeal grinding of bacteria	
Misc.			
	kat-1	fat storage; suppressed by skat-1	Mak et. al., 2006

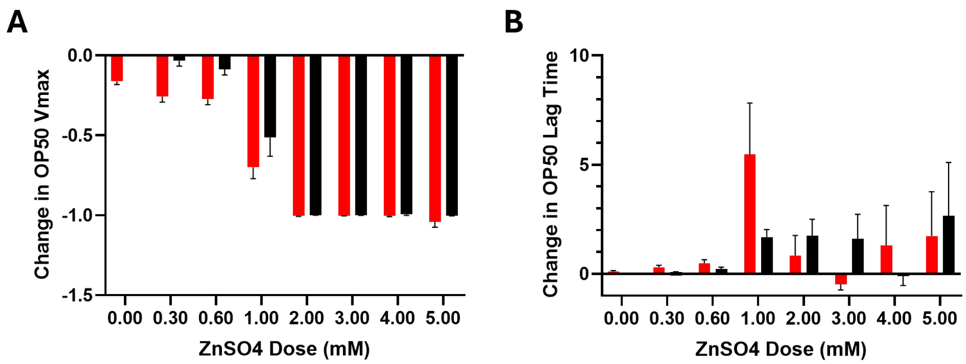

Supp. Figure 1. Impact of 3HAA and zinc treatment on *E. coli* growth in liquid culture at higher doses.
(A) Change in max velocity in *E. coli* treated with increasing zinc doses with and without 1 mM 3HAA treatment. Both treatments show a decrease in Vmax up to 2 mM. **(B)** Change in lag time in *E. coli* treated with increasing zinc doses with and without 1 mM 3HAA treatment. Both treatments show an increase in lag that does not appear to be dose dependent. Data represents 3 biological replicates per treatment. All conditions normalized to untreated *E. coli* control. Zinc sulfate doses in black, zinc sulfate doses with 1 mM 3HAA treatment in red.

REFERENCES

1. Dang, H., Castro-Portuguez, R., Espejo, L., Backer, G., Freitas, S., Spence, E., Meyers, J., Shuck, K., Gardea, E. A., Chang, L. M., Balsa, J., Thorns, N., Corban, C., Liu, T., Bean, S., Sheehan, S., Korstanje, R., & Sutphin, G. L. (2023). On the benefits of the tryptophan metabolite 3-hydroxyanthranilic acid in Caenorhabditis elegans and mouse aging. *Nature Communications*, *14*(1), 8338. https://doi.org/10.1038/s41467-023-43527-1
2. *Underlying Cause of Death, 2018-2021, Single Race Results Form*. (n.d.). Retrieved March 13, 2024, from https://wonder.cdc.gov/controller/datarequest/D158;jsessionid=A1E9A4BCA79F38854887648636CF
3. Sadighi Akha, A. A. (2018). Aging and the immune system: An overview. *Journal of Immunological Methods*, *463*, 21–26. https://doi.org/10.1016/j.jim.2018.08.005
4. López-Otín, C., Blasco, M. A., Partridge, L., Serrano, M., & Kroemer, G. (2013). The Hallmarks of Aging. *Cell*, *153*(6), 1194–1217. https://doi.org/10.1016/j.cell.2013.05.039
5. López-Otín, C., Blasco, M. A., Partridge, L., Serrano, M., & Kroemer, G. (2023). Hallmarks of aging: An expanding universe. *Cell*, *186*(2), 243–278. https://doi.org/10.1016/j.cell.2022.11.001
6. Crimmins, E. M. (2015). Lifespan and Healthspan: Past, Present, and Promise. *The Gerontologist*, *55*(6), 901–911. https://doi.org/10.1093/geront/gnv130
7. Kaeberlein, M. (2018). How healthy is the healthspan concept? *GeroScience*, *40*(4), 361–364. https://doi.org/10.1007/s11357-018-0036-9
8. Franceschi, C., & Campisi, J. (2014). Chronic Inflammation (Inflammaging) and Its Potential Contribution to Age-Associated Diseases. *The Journals of Gerontology: Series A*, *69*(Suppl_1), S4–S9. https://doi.org/10.1093/gerona/glu057
9. Pawelec, G. (2018). Age and immunity: What is "immunosenescence"? *Experimental Gerontology*, *105*, 4–9. https://doi.org/10.1016/j.exger.2017.10.024
10. Meneely, P. M., Dahlberg, C. L., & Rose, J. K. (2019). Working with Worms: Caenorhabditis elegans as a Model Organism. *Current Protocols Essential Laboratory Techniques*, *19*(1), e35. https://doi.org/10.1002/cpet.35
11. Henricson, A., Sonnhammer, E. L., Baillie, D. L., & Gomes, A. V. (2004). Functional characterization in Caenorhabditis elegans of transmembrane worm-human orthologs. *BMC Genomics*, *5*(1), 85. https://doi.org/10.1186/1471-2164-5-85

12. Grishok, A. (2005). RNAi mechanisms in *Caenorhabditis elegans*. *FEBS Letters*, *579*(26), 5932–5939. https://doi.org/10.1016/j.febslet.2005.08.001

13. Wang, C., Xia, C., Zhu, Y., & Zhang, H. (2021). Innovative fluorescent probes for in vivo visualization of biomolecules in living Caenorhabditis elegans. *Cytometry Part A*, *99*(6), 560–574. https://doi.org/10.1002/cyto.a.24325

14. Ermolaeva, M. A., & Schumacher, B. (2014). Insights from the worm: The *C. elegans* model for innate immunity. *Seminars in Immunology*, *26*(4), 303–309. https://doi.org/10.1016/j.smim.2014.04.005

15. Seiler, F., Hellberg, J., Lepper, P. M., Kamyschnikow, A., Herr, C., Bischoff, M., Langer, F., Schäfers, H.-J., Lammert, F., Menger, M. D., Bals, R., & Beisswenger, C. (2013). FOXO Transcription Factors Regulate Innate Immune Mechanisms in Respiratory Epithelial Cells. *The Journal of Immunology*, *190*(4), 1603–1613. https://doi.org/10.4049/jimmunol.1200596

16. Arthur, J. S. C., & Ley, S. C. (2013). Mitogen-activated protein kinases in innate immunity. *Nature Reviews Immunology*, *13*(9), 679–692. https://doi.org/10.1038/nri3495

17. Travis, M. A., & Sheppard, D. (2014). TGF-β Activation and Function in Immunity. *Annual Review of Immunology*, *32*(Volume 32, 2014), 51–82. https://doi.org/10.1146/annurev-immunol-032713-120257

18. Kim, B.-J., Lee, S. H., & Koh, J.-M. (2020). Clinical insights into the kynurenine pathway in age-related diseases. *Experimental Gerontology*, *130*, 110793. https://doi.org/10.1016/j.exger.2019.110793

19. Castro-Portuguez, R., & Sutphin, G. L. (2020). Kynurenine pathway, NAD+ synthesis, and mitochondrial function: Targeting tryptophan metabolism to promote longevity and healthspan. *Experimental Gerontology*, *132*, 110841. https://doi.org/10.1016/j.exger.2020.110841

20. Badawy, A. A.-B. (2017). Kynurenine Pathway of Tryptophan Metabolism: Regulatory and Functional Aspects. *International Journal of Tryptophan Research : IJTR*, *10*, 1178646917691938. https://doi.org/10.1177/1178646917691938

21. Oxenkrug, G. F. (2010). The extended life span of Drosophila melanogaster eye-color (white and vermilion) mutants with impaired formation of kynurenine. *Journal of Neural Transmission (Vienna, Austria : 1996)*, *117*(1), 23–26. https://doi.org/10.1007/s00702-009-0341-7

22. Oxenkrug, G., Navrotskaya, V., Vorobyova, L., & Summergrad, P. (2011). Extension of life span of Drosophila melanogaster by the inhibitors of tryptophan-kynurenine metabolism. *Fly*, *5*(4), 307–309. https://doi.org/10.4161/fly.5.4.18414

23. van der Goot, A. T., Zhu, W., Vazquez-Manrique, R. P., Seinstra, R. I., Dettmer, K., Michels, H., Farina, F., Krijnen, J., Melki, R., Buijsman, R. C., Ruiz Silva, M., Thijssen, K. L., Kema, I. P., Neri, C., Oefner, P. J., & Nollen, E. A. A. (2012). Delaying aging and the aging-associated decline in protein homeostasis by inhibition of tryptophan degradation. *Proceedings of the National Academy of Sciences*, *109*(37), 14912–14917. https://doi.org/10.1073/pnas.1203083109

24. Sutphin, G. L., Backer, G., Sheehan, S., Bean, S., Corban, C., Liu, T., Peters, M. J., van Meurs, J. B. J., Murabito, J. M., Johnson, A. D., & Korstanje, R. (2017). Caenorhabditis elegans orthologs of human genes differentially expressed with age are enriched for determinants of longevity. *Aging Cell*, *16*(4), 672–682. https://doi.org/10.1111/acel.12595

25. Katsyuba, E., Mottis, A., Zietak, M., De Franco, F., van der Velpen, V., Gariani, K., Ryu, D., Cialabrini, L., Matilainen, O., Liscio, P., Giacchè, N., Stokar-Regenscheit, N., Legouis, D., de Seigneux, S., Ivanisevic, J., Raffaelli, N., Schoonjans, K., Pellicciari, R., & Auwerx, J. (2018). De novo NAD+ synthesis enhances mitochondrial function and improves health. *Nature*, *563*(7731), 354–359. https://doi.org/10.1038/s41586-018-0645-6

26. Dang, H., Castro-Portuguez, R., Espejo, L., Backer, G., Freitas, S., Spence, E., Meyers, J., Shuck, K., Corban, C., Liu, T., Bean, S., Sheehan, S., Korstanje, R., & Sutphin, G. L. (2021). *3-hydroxyanthranilic acid – a new metabolite for healthy lifespan extension* (p. 2021.06.01.446651). bioRxiv. https://doi.org/10.1101/2021.06.01.446651

27. Espejo, L. S., DeNicola, D., Chang, L. M., Hofschneider, V., Haskins, A. E., Balsa, J., Freitas, S. S., Antenor, A., Hamming, S., Hull, B., Castro-Portuguez, R., Dang, H., & Sutphin, G. L. (2024). The Emerging Role of 3-Hydroxyanthranilic Acid on C. elegans Aging Immune Function. *bioRxiv*, 2024.01.07.574394. https://doi.org/10.1101/2024.01.07.574394

28. Balla, K. M., & Troemel, E. R. (2013). Caenorhabditis elegans as a model for intracellular pathogen infection. *Cellular Microbiology*, *15*(8), 1313–1322. https://doi.org/10.1111/cmi.12152

29. Clokey, G. V., & Jacobson, L. A. (1986). The autofluorescent “lipofuscin granules” in the intestinal cells of *Caenorhabditis elegans* are secondary lysosomes. *Mechanisms of Ageing and Development*, *35*(1), 79–94. https://doi.org/10.1016/0047-6374(86)90068-0

30. Hajdú, G., Somogyvári, M., Csermely, P., & Sőti, C. (2023). Lysosome-related organelles promote stress and immune responses in C. elegans. *Communications Biology*, *6*(1), 936. https://doi.org/10.1038/s42003-023-05246-7

31. Coburn, C., Allman, E., Mahanti, P., Benedetto, A., Cabreiro, F., Pincus, Z., Matthijssens, F., Araiz, C., Mandel, A., Vlachos, M., Edwards, S.-A., Fischer, G., Davidson, A., Pryor, R. E., Stevens, A., Slack,

F. J., Tavernarakis, N., Braeckman, B. P., Schroeder, F. C., … Gems, D. (2013). Anthranilate Fluorescence Marks a Calcium-Propagated Necrotic Wave That Promotes Organismal Death in C. elegans. *PLOS Biology*, *11*(7), e1001613. https://doi.org/10.1371/journal.pbio.1001613

32. Roh, H. C., Collier, S., Guthrie, J., Robertson, J. D., & Kornfeld, K. (2012). Lysosome-Related Organelles in Intestinal Cells Are a Zinc Storage Site in C. elegans. *Cell Metabolism*, *15*(1), 88–99. https://doi.org/10.1016/j.cmet.2011.12.003
33. Earley, B. J., Mendoza, A. D., Tan, C.-H., & Kornfeld, K. (2021). Zinc homeostasis and signaling in the roundworm *C. elegans*. *Biochimica et Biophysica Acta (BBA) - Molecular Cell Research*, *1868*(1), 118882. https://doi.org/10.1016/j.bbamcr.2020.118882
34. Selvapandiyan, A., Puri, N., Kumar, P., Alam, A., Ehtesham, N. Z., Griffin, G., & Hasnain, S. E. (2023). Zooming in on common immune evasion mechanisms of pathogens in phagolysosomes: Potential broad-spectrum therapeutic targets against infectious diseases. *FEMS Microbiology Reviews*, *47*(1), fuac041. https://doi.org/10.1093/femsre/fuac041
35. Hu, W., Chan, H., Lu, L., Wong, K. T., Wong, S. H., Li, M. X., Xiao, Z. G., Cho, C. H., Gin, T., Chan, M. T. V., Wu, W. K. K., & Zhang, L. (2020). Autophagy in intracellular bacterial infection. *Seminars in Cell & Developmental Biology*, *101*, 41–50. https://doi.org/10.1016/j.semcdb.2019.07.014
36. Barrett, A., & Hermann, G. J. (2016). A Caenorhabditis elegans Homologue of LYST Functions in Endosome and Lysosome-Related Organelle Biogenesis. *Traffic*, *17*(5), 515–535. https://doi.org/10.1111/tra.12381
37. Cullinane, A. R., Schäffer, A. A., & Huizing, M. (2013). The BEACH Is Hot: A LYST of Emerging Roles for BEACH-Domain Containing Proteins in Human Disease. *Traffic*, *14*(7), 749–766. https://doi.org/10.1111/tra.12069
38. Gkikas, I., Daskalaki, I., Kounakis, K., Tavernarakis, N., & Lionaki, E. (2023). MitoSNARE Assembly and Disassembly Factors Regulate Basal Autophagy and Aging in C. elegans. *International Journal of Molecular Sciences*, *24*(4), Article 4. https://doi.org/10.3390/ijms24044230
39. Teng, F. Y. H., Wang, Y., & Tang, B. L. (2001). The syntaxins. *Genome Biology*, *2*(11), reviews3012.1. https://doi.org/10.1186/gb-2001-2-11-reviews3012
40. *WormBase: Nematode Information Resource*. (n.d.). Retrieved April 11, 2024, from https://wormbase.org/#012-34-5
41. Rolfe, M. D., Rice, C. J., Lucchini, S., Pin, C., Thompson, A., Cameron, A. D. S., Alston, M., Stringer, M. F., Betts, R. P., Baranyi, J., Peck, M. W., & Hinton, J. C. D. (2012). Lag Phase Is a Distinct Growth

Phase That Prepares Bacteria for Exponential Growth and Involves Transient Metal Accumulation. *Journal of Bacteriology*, *194*(3), 686–701. https://doi.org/10.1128/jb.06112-11

42. Luis S Espejo, Samuel Freitas, Vanessa Silbar, Leah Chang, Jonah Balsa, Angelo Antenor, Hope Dang, Destiny DeNicola, & George L Sutphin. (2023). SICKO: Systematic Imaging of Caenorhabditis Killing Organisms. *bioRxiv*, 2023.02.17.529009. https://doi.org/10.1101/2023.02.17.529009
43. Espejo, L., Hull, B., Chang, L. M., DeNicola, D., Freitas, S., Silbar, V., Haskins, A., Turner, E. A., & Sutphin, G. L. (2022). Long-Term Culture of Individual Caenorhabditis elegans on Solid Media for Longitudinal Fluorescence Monitoring and Aversive Interventions. *JoVE (Journal of Visualized Experiments)*, *190*, e64682. https://doi.org/10.3791/64682
44. Cukierman, E., Huber, I., Rotman, M., & Cassel, D. (1995). The ARF1 GTPase-Activating Protein: Zinc Finger Motif and Golgi Complex Localization. *Science*, *270*(5244), 1999–2002. https://doi.org/10.1126/science.270.5244.1999
45. Berg, M., Polyzos, K. A., Agardh, H., Baumgartner, R., Forteza, M. J., Kareinen, I., Gisterå, A., Bottcher, G., Hurt-Camejo, E., Hansson, G. K., & Ketelhuth, D. F. J. (2020). 3-Hydroxyanthralinic acid metabolism controls the hepatic SREBP/lipoprotein axis, inhibits inflammasome activation in macrophages, and decreases atherosclerosis in Ldlr−/− mice. *Cardiovascular Research*, *116*(12), 1948–1957. https://doi.org/10.1093/cvr/cvz258
46. Shi, Z., Gan, G., Gao, X., Chen, F., & Mi, J. (2021). *3-HAA Metabolic Pathway Regulates HCC Growth*. https://doi.org/10.21203/rs.3.rs-898525/v1
47. Sutphin, G. L., & Kaeberlein, M. (2009). Measuring Caenorhabditis elegans Life Span on Solid Media. *Journal of Visualized Experiments : JoVE*, *27*, 1152. https://doi.org/10.3791/1152
48. Fares, H., & Greenwald, I. (2001). Regulation of endocytosis by CUP-5, the Caenorhabditis elegans mucolipin-1 homolog. *Nature Genetics*, *28*(1), 64–68. https://doi.org/10.1038/ng0501-64
49. *TBC-2 Regulates RAB-5/RAB-7-mediated Endosomal Trafficking in Caenorhabditis elegans | Molecular Biology of the Cell*. (n.d.). Retrieved April 11, 2024, from https://www.molbiolcell.org/doi/full/10.1091/mbc.e09-11-0947
50. *RAB-6.1 and RAB-6.2 Promote Retrograde Transport in C. elegans | PLOS ONE*. (n.d.). Retrieved April 11, 2024, from https://journals.plos.org/plosone/article?id=10.1371/journal.pone.0149314
51. Soukas, A. A., Carr, C. E., & Ruvkun, G. (2013). Genetic Regulation of Caenorhabditis elegans Lysosome Related Organelle Function. *PLOS Genetics*, *9*(10), e1003908. https://doi.org/10.1371/journal.pgen.1003908

52. *Cation Diffusion Facilitator Gene cdf-2 Mediates Zinc Metabolism in Caenorhabditis elegans | Genetics | Oxford Academic*. (n.d.). Retrieved April 11, 2024, from https://academic.oup.com/genetics/article/182/4/1015/6081163

53. Rabbitts, B. M., Ciotti, M. K., Miller, N. E., Kramer, M., Lawrenson, A. L., Levitte, S., Kremer, S., Kwan, E., Weis, A. M., & Hermann, G. J. (2008). Glo-3, a Novel Caenorhabditis elegans Gene, Is Required for Lysosome-Related Organelle Biogenesis. *Genetics*, *180*(2), 857–871. https://doi.org/10.1534/genetics.108.093534

54. Parker, S., Walker, D. S., Ly, S., & Baylis, H. A. (2009). Caveolin-2 Is Required for Apical Lipid Trafficking and Suppresses Basolateral Recycling Defects in the Intestine of Caenorhabditis elegans. *Molecular Biology of the Cell*, *20*(6), 1763–1771. https://doi.org/10.1091/mbc.e08-08-0837

55. Williams, T. M., & Lisanti, M. P. (2004). The caveolin proteins. *Genome Biology*, *5*(3), 214. https://doi.org/10.1186/gb-2004-5-3-214

56. Chen, S., Li, L., Li, J., Liu, B., Zhu, X., Zheng, L., Zhang, R., & Xu, T. (2014). SEC-10 and RAB-10 coordinate basolateral recycling of clathrin-independent cargo through endosomal tubules in Caenorhabditis elegans. *Proceedings of the National Academy of Sciences*, *111*(43), 15432–15437. https://doi.org/10.1073/pnas.1408327111

57. Morris, C., Foster, O. K., Handa, S., Peloza, K., Voss, L., Somhegyi, H., Jian, Y., Vo, M. V., Harp, M., Rambo, F. M., Yang, C., & Hermann, G. J. (2018). Function and regulation of the Caenorhabditis elegans Rab32 family member GLO-1 in lysosome-related organelle biogenesis. *PLOS Genetics*, *14*(11), e1007772. https://doi.org/10.1371/journal.pgen.1007772

58. Currie, E., King, B., Lawrenson, A. L., Schroeder, L. K., Kershner, A. M., & Hermann, G. J. (2007). Role of the Caenorhabditis elegans Multidrug Resistance Gene, mrp-4, in Gut Granule Differentiation. *Genetics*, *177*(3), 1569–1582. https://doi.org/10.1534/genetics.107.080689

59. Tan, C.-H., Wang, T.-Y., Park, H., Lomenick, B., Chou, T.-F., & Sternberg, P. W. (2023). *Single tissue proteomics in Caenorhabditis elegans reveals proteins resident in intestinal lysosome-related organelles* (p. 2023.12.29.573592). bioRxiv. https://doi.org/10.1101/2023.12.29.573592

60. Schroeder, L. K., Kremer, S., Kramer, M. J., Currie, E., Kwan, E., Watts, J. L., Lawrenson, A. L., & Hermann, G. J. (2007). Function of the Caenorhabditis elegans ABC Transporter PGP-2 in the Biogenesis of a Lysosome-related Fat Storage Organelle. *Molecular Biology of the Cell*, *18*(3), 995–1008. https://doi.org/10.1091/mbc.e06-08-0685

61. *GOP-1 promotes apoptotic cell degradation by activating the small GTPase Rab2 in C. elegans | Journal of Cell Biology | Rockefeller University Press*. (n.d.). Retrieved April 11, 2024, from https://rupress.org/jcb/article/216/6/1775/38963/GOP-1-promotes-apoptotic-cell-degradation-by

62. Mack, H. I. D., Kremer, J., Albertini, E., Mack, E. K. M., & Jansen-Dürr, P. (2022). Regulation of fatty acid desaturase- and immunity gene-expression by mbk-1/DYRK1A in Caenorhabditis elegans. *BMC Genomics*, *23*(1), 25. https://doi.org/10.1186/s12864-021-08176-y

63. *Vacuolar protein sorting protein 41 (VPS41) at an intersecti... : Neural Regeneration Research*. (n.d.). Retrieved April 11, 2024, from https://journals.lww.com/nrronline/fulltext/2019/14070/vacuolar_protein_sorting_protein_41__vps41__at_an.17.aspx

64. Brandt, J. N., Voss, L., Rambo, F. M., Nicholson, K., Thein, J. R., Fairchild, L., Seabrook, L., Lewis, D., Guevara-Hernandez, L., White, M. L., Sax, L., Eichten, V., Harper, L., & Hermann, G. J. (2022). Asymmetric organelle positioning during epithelial polarization of *C. elegans* intestinal cells. *Developmental Biology*, *481*, 75–94. https://doi.org/10.1016/j.ydbio.2021.09.007